NANO LETTERS

Letter

pubs.acs.org/NanoLett

Nanoscale Control of Rewriteable Doping Patterns in Pristine Graphene/Boron Nitride Heterostructures

Jairo Velasco Jr.,[†,⊥] Long Ju,[†] Dillon Wong,[†] Salman Kahn,[†] Juwon Lee,[†] Hsin-Zon Tsai,[†] Chad Germany,[†] Sebastian Wickenburg,[†] Jiong Lu,[†] Takashi Taniguchi,[∥] Kenji Watanabe,[∥] Alex Zettl,[†,‡,§] Feng Wang,[†,‡,§] and Michael F. Crommie*[,†,‡,§]

[†]Department of Physics, University of California, Berkeley, California 94720, United States

[‡]Materials Sciences Division, Lawrence Berkeley National Laboratory, Berkeley, California 94720, United States

[§]Kavli Energy NanoSciences Institute at the University of California, Berkeley and the Lawrence Berkeley National Laboratory, Berkeley, California 94720, United States

[∥]National Institute for Materials Science, 1-1 Namiki, Tsukuba, 305-0044, Japan

[⊥]Department of Physics, University of California, Santa Cruz, California 95064, United States

Supporting Information

ABSTRACT: Nanoscale control of charge doping in two-dimensional (2D) materials permits the realization of electronic analogs of optical phenomena, relativistic physics at low energies, and technologically promising nanoelectronics. Electrostatic gating and chemical doping are the two most common methods to achieve local control of such doping. However, these approaches suffer from complicated fabrication processes that introduce contamination, change material properties irreversibly, and lack flexible pattern control. Here we demonstrate a clean, simple, and reversible technique that permits writing, reading, and erasing of doping patterns for 2D materials at the nanometer scale. We accomplish this by employing a graphene/boron nitride heterostructure that is equipped with a bottom gate electrode. By using electron transport and scanning tunneling microscopy (STM), we demonstrate that spatial control of charge doping can be realized with the application of either light or STM tip voltage excitations in conjunction with a gate electric field. Our straightforward and novel technique provides a new path toward on-demand graphene p−n junctions and ultrathin memory devices.

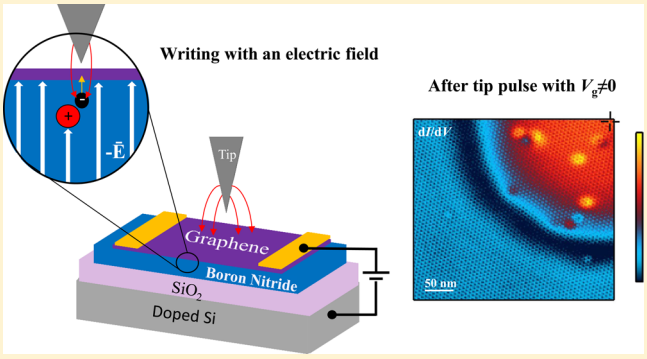

KEYWORDS: *Graphene/boron nitride heterostructures, scanning tunneling microscopy, p−n junctions, boron nitride defects*

Local control of charge doping in 2D systems allows for the study of new classes of phenomena that include electronic lensing,[1,2] Klein tunneling,[3,4] ultrathin light emitting diodes,[5−7] and in situ tunable plasmonic platforms.[8] The fabrication of nanostructures exhibiting such doping, however, requires sophisticated lithography procedures that compromise sample quality and do not yield flexible control of doping patterns,[9−14] thus hampering advancement in these areas. Some progress has been made in patterning buried GaAs/AlGaAs heterojunctions via a lithography-free conducting AFM tip-based technique[15] although only for a single dopant polarity. For more open graphene/BN heterostructures, it has been shown that illumination via visible light causes defect charge migration within the BN layer, thus shifting the graphene charge neutrality point (CNP)[16] and inducing doping. Currently, however, there is no understanding of how such defect charge migration varies spatially at the nanoscale and whether it might be exploited as a tool for developing new 2D devices.

Here we address these issues directly via a new scheme that combines optical and local electric field excitation of defect charge in a BN insulator overlaid with graphene. This permits us to write, read, and even erase doping patterns at the nanoscale. Unlike other tip-based patterning methods,[15] this new technique allows direct wave function mapping of 2D devices and control over local doping polarity. Figure 1 shows two different schemes that we used for creating our rewritable doping patterns in a graphene/BN heterostructure supported by an SiO_2/Si substrate and contacted by gold/chrome electrodes. A backgate voltage V_g applied to the doped Si substrate permits global tuning of the graphene doping level, while local modification is achieved by excitation (via photons or DC electric field) of electrons (holes) from donor-like

Received: November 1, 2015
Revised: January 31, 2016
Published: February 8, 2016

DOI: 10.1021/acs.nanolett.5b04441
Nano Lett. 2016, 16, 1620−1625

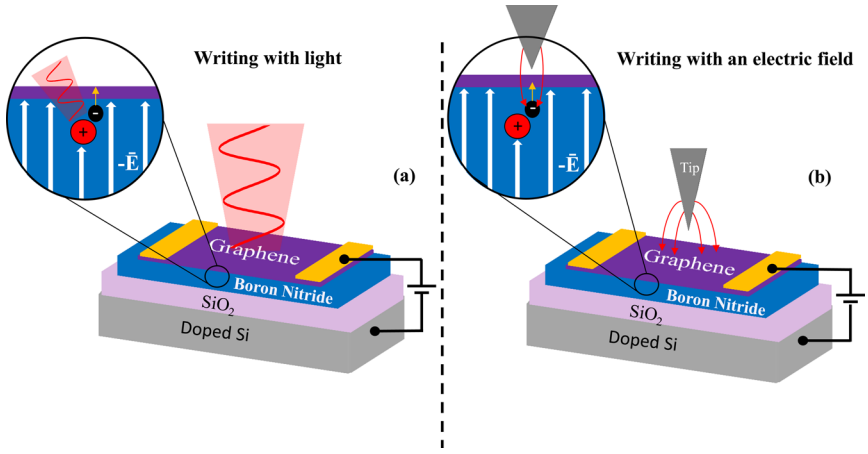

Figure 1. Scheme for creating rewritable nanoscale doping patterns on graphene/BN heterostructures. (a) Light-based scheme: graphene/BN heterostructure supported by SiO_2/Si substrate. The graphene is contacted by gold electrodes and a backgate voltage V_g is applied to the doped Si substrate. A doping pattern is induced in the sample by exposing it to light for a short period while holding $V_g \neq 0$ V. (b) Tip-based scheme: device structure is the same as in (a). Here a doping pattern is induced by applying a voltage pulse to the tip while holding $V_g \neq 0$ V. Erasing is accomplished by either light-based or tip-based excitation while holding $V_g = 0$ V.

(acceptor-like) defects in BN. The liberated charge leaves behind ions that locally gate the graphene layer above (this is equivalent to doping for graphene). Figure 1a,b depicts this process for a donor-like defect via optical excitation (Figure 1a) and tip-induced electric field (Figure 1b).

We first explore microscopic spatial fluctuations in defect charge doping induced by light. Figure 2a shows the result of transport measurements (σ vs V_g) taken on our graphene/BN heterostructure after different light exposures. The response of the device prior to light exposure is shown in the red trace and is referred to as State 1. Here the dip in σ (which marks the CNP) is located at $V_g \sim 0$ V. The narrow width of the CNP dip is evidence that the sample starts off with a low amount of spatial fluctuations in the underlying charge landscape of the BN substrate.[17] We then set the gate to $V_g = -38$ V and exposed the sample to light for ~45 s (λ = 405 nm, power density ~10 μW μm^{-2}). The $\sigma(V_g)$ curve measured immediately afterward (with the light off) is shown in the green trace and is referred to as State 2. Here we see that the CNP dip is much wider and has shifted to $V_g \sim -15$ V. Next we exposed the device to light for a significantly longer period (~10 min) with the gate again held at $V_g = -38$ V. The $\sigma(V_g)$ measurement performed afterward is shown as the blue trace and is referred to as State 3. The CNP dip is now seen to have narrowed to its original width but it is shifted to $V_g = -38$ V, precisely the value of the gate voltage during the light exposure.

The differences in shape between the three $\sigma(V_g)$ curves provide evidence of a microscopic doping pattern induced by light exposure. The broadened width for State 2 indicates that it has a different doping landscape compared to State 1, an enhancement in charge inhomogeneity.[18] We attribute this change to light-induced redistribution of charged impurities in the BN substrate. Optically excited electrons from defect sites (that are distributed randomly within the BN crystal) migrate both to the graphene and to other randomly distributed defects under the influence of the gate electric field and homogeneous illumination. Short light exposure (i.e., where defect charge migration is insufficient to fully screen the gate potential) leads to a disordered distribution of the overall charged defects that increase charge inhomogeneity within the graphene, thus widening $\sigma(V_g)$ (as seen in State 2). Upon further light exposure, the charged defects form a more even distribution in order to fully screen the gate-induced electric field in the BN, thus "erasing" the charge inhomogeneity induced by the shorter light exposure (as evidenced by State 3). Closer inspection of our transport measurements for States 1−3 further support the emergence of a microscopic doping pattern induced by light. This can be seen in Figure 2b where the electron branch of the $\sigma(V_g)$ curves are replotted as $\sigma(n)$ with n on a logarithmic scale. Here the average amplitude of the charge inhomogeneity in graphene is measured by the point of intersection of the two lines extending from the constant sloped regions.[19] This is marked by colored arrows for each curve. For State 2, the charge inhomogeneity amplitude is larger by an order of magnitude than States 1 and 3 and so reveals a doping landscape patterned by light.

In order to directly visualize the nanoscale characteristics of this doping pattern, we performed STM measurements on our graphene/BN heterostructure after different optical treatments. Figure 2c−e shows differential conductance (dI/dV) maps obtained at constant sample bias V_s and gate voltage $\tilde{V}_g$ ($\tilde{V}_g$ denotes the gate voltage applied during a dI/dV measurement while V_g denotes the gate voltage applied during exposure of the sample to light or a voltage pulse). These measurements were performed at the same location both before and after light exposures similar to those discussed in Figure 2a,b. All maps exhibited a 7 nm moiré pattern, indicating a clean graphene/BN interface. Before any light exposure (Figure 2c) we observe low spatial variation in the dI/dV intensity, except for a single charged defect visible as a red dot in the lower right quadrant of the map.[20] Next, we retracted the tip, set $V_g = -15$ V, and exposed the device to a short light exposure of 20 s (similar to how State 2 was prepared in Figure 2a). As seen in Figure 2d, the resulting dI/dV map exhibits significant new charge inhomogeneity, observable as an irregularly shaped red area in the top right portion of the map. We then retracted the tip, set $V_g = -15$ V, and performed a long light exposure for 15 min on the device (similar to how State 3 was prepared in Figure 2a). As seen in Figure 2e, this erases the charge inhomogeneity and reduces it to the same level as observed for the pristine sample in Figure 2c. The sequence of observations in Figure

DOI: 10.1021/acs.nanolett.5b04441
Nano Lett. 2016, 16, 1620−1625

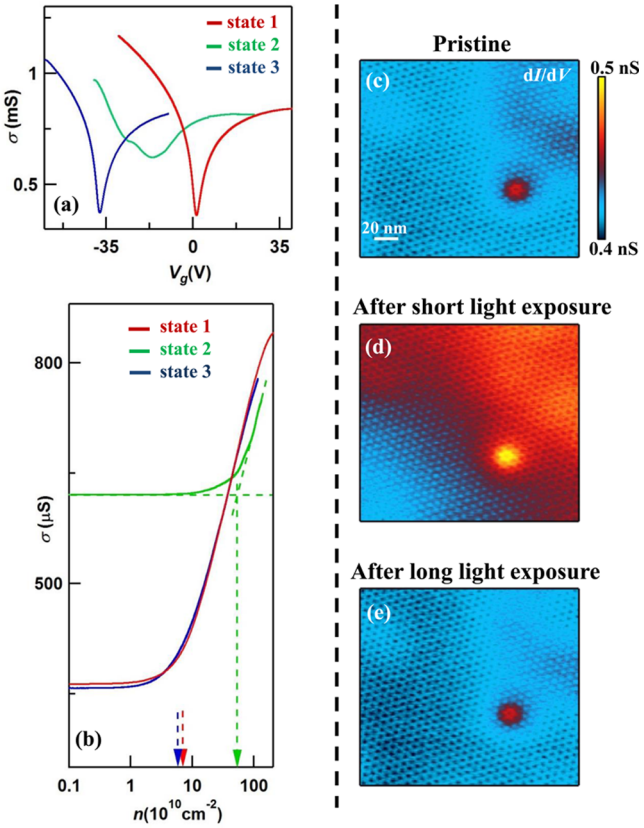

Figure 2. Nanoscale charge inhomogeneity controlled with light. (a) $\sigma(V_g)$ curves obtained after different light exposures. Red trace: pristine sample. Green trace: acquired after a short light exposure (45 s) while holding $V_g = -38$ V. Blue trace: acquired after extended light exposure (10 min) while holding $V_g = -38$ V. (b) $\sigma(n)$ curves (with n plotted on a logarithmic scale) indicate the amplitude of charge inhomogeneity, δn (denoted by the colored arrows) from (a). Data from (a,b) were acquired from a device with a 9 μm width and 2 μm source-drain separation. (c) The dI/dV map of pristine graphene/BN ($I = 0.2$ nA, $V_s = -0.25$ V, $\tilde{V}_g = 5$ V). $\tilde{V}_g$ denotes the gate voltage applied during the acquisition of a dI/dV map. (d) The dI/dV map of the same region after a short light exposure (20 s), while holding $V_g = -15$ V (acquired with $\tilde{V}_g = -10$ V and same I and V_s as (c)). (e) The dI/dV map of the same region after extended light exposure (15 min) while holding $V_g = -15$ V (acquired with $\tilde{V}_g = -13$ V and same I and V_s as (c)). ($\tilde{V}_g$ is slightly different for each dI/dV map so that they could all be acquired at the same global charge density). Data from (c–e) were acquired from a device with a 44 μm width and 39 μm source-drain separation.

2c–e was replicated at numerous locations with many tips and with different devices.

The changes observed in our dI/dV maps provide a direct visualization of how the doping landscape can be tuned by light excitation. Because variations in dI/dV are proportional to changes in the electronic local density of states, dI/dV maps taken at a fixed bias near graphene's Dirac point (DP) reflect spatial variation in the DP energy.[21,22] Such images can be converted to a charge density fluctuation amplitude δn in a straightforward way (see Figure S1). The small variations in dI/dV intensity of Figure 2c (the image prior to light exposure) indicate a small δn ($\sim 10^9$ cm^{-2}), consistent with previous STM studies of graphene/BN heterostructures.[23,24] The charge density fluctuations seen in Figure 2d (after a short light exposure), however, reflect much larger charge fluctuations ($\delta n \sim 10^{10}$ cm^{-2} across the image). This is consistent with the broadened CNP feature observed in the transport measurement of State 2 (Figure 2a). The reduction of charge inhomogeneity seen in the spatial map of Figure 2e after long light exposure is consistent with the narrowing of the CNP feature observed via a transport measurement of State 3 after similar processing (Figure 2a). Both the dI/dV maps and the transport data support a light-induced charge doping mechanism where optical excitation frees defect charge in the insulating layer that then migrates in response to the gate electric field. Here nanoscale inhomogeneity arises from spatial disorder in the BN defect density, which causes transient fluctuations in the local graphene charge carrier density as the defect charge rearranges itself to screen the backgate field.

These light-induced doping patterns emerge at arbitrary positions because the BN defects (the source of the migrating charge within the BN) are randomly located throughout the BN crystal. A natural question to ask is whether this defect-mediated charge migration process might be harnessed and controlled locally with more precision. A recent experiment found that individual defects in BN can be ionized by STM tip voltage pulses,[20] but that experiment was performed in the absence of a gate electric field (unlike the experiments discussed here) and detected no net charge exchange between graphene and the insulating substrate. To test the effect of a local ionizing potential on defect charge migration in the presence of a gate electric field, we applied tip voltage pulses to a graphene/BN device using the experimental setup sketched in Figure 1b. Figure 3a shows dI/dV spectra obtained with $\tilde{V}_g = 0$ V after applying $V_s = 5$ V tip voltage pulses while holding V_g at different values (the dI/dV spectra were obtained at the same location the tip pulses were applied). The red trace shows the reference spectrum measured before application of any tip pulses. Here we observe an ~130 mV gaplike feature at the Fermi energy[24,25] that is known to arise due to phonon-mediated inelastic tunneling.[25] To the right of this inelastic tunneling feature is a dip (black arrow) that marks the DP. Because the DP lies to the right of the Fermi energy ($V_s = 0$ V), we see that this region of the surface has residual p-doping ($\sim 5 \times 10^{11}$ cm^{-2}) at zero gate voltage. The yellow, green, and blue traces show the dI/dV spectra measured after applying tip pulses lasting 30 s with the gate voltage set respectively to $V_g = -10$, -20, and -30 V (the height of the tip in each case was approximately 1.5 nm away from the surface, see Supporting Information for details). As shown by the black arrows, the DP shifts down in energy as each tip pulse is delivered with a more negative gate voltage. The sample is seen to locally change from p-type doping to n-type doping after the first pulse and then to become more heavily n-doped after each pulse. This behavior is consistent with the local BN charge landscape becoming increasingly positively charged after tip pulses performed at increasingly negative gate voltages. Reversing the polarity of the gate field, while leaving everything else the same, results in local graphene doping with the exact opposite polarity (see Figure S2).

We were able to gain insight into the spatially varying dopant landscape that results from a tip pulse by performing dI/dV imaging of the area beneath the STM tip both before and after a tip pulse. All maps exhibited a 7 nm moiré pattern, indicating a clean graphene/BN interface. Figure 3b shows a dI/dV map of a patch of graphene right before performing a tip pulse. It contains a number of point-like defects due to charge centers in the BN layer[20] but otherwise exhibits a smooth charge

DOI: 10.1021/acs.nanolett.5b04441
Nano Lett. 2016, 16, 1620–1625

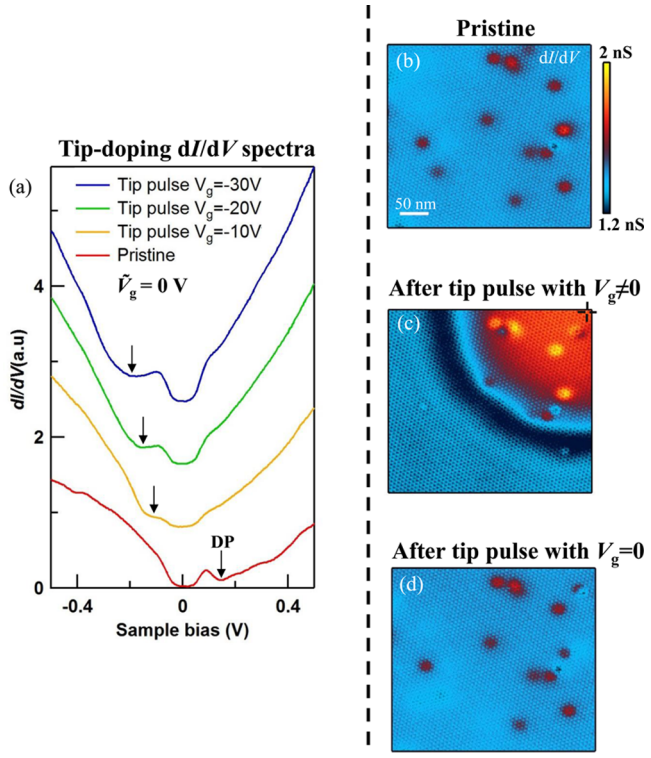

Figure 3. Nanoscale doping patterns controlled with an STM tip voltage pulse. (a) The dI/dV spectroscopy of a pristine surface before a tip pulse (red) and after a tip pulse (V_s = 5 V, 30 s) for V_g = −10 V (yellow), −20 V (green), and −30 V (blue). Initial tunneling parameters: I = 0.4 nA, V_s = −0.5 V, $\tilde{V}_g$ = 0. The curves are vertically offset for clarity. (b) dI/dV map of pristine graphene/BN (I = 0.4 nA, V_s = −0.25 V, $\tilde{V}_g$ = 5 V). (c) The dI/dV map of the same region after a tip pulse was applied in the corner of the map (location denoted by cross hair), while holding V_g = −20 V (I = 0.4 nA, V_s = −0.25 V, $\tilde{V}_g$ = −10 V). (d) The dI/dV map of the same region after another tip pulse was applied in the same location, while holding V_g = 0 V (I = 0.4 nA, V_s = −0.25 V, $\tilde{V}_g$ = 5 V). All data were acquired from a device with a 44 μm width and 39 μm source-drain separation.

landscape. We next brought the STM tip to the top right corner of this region and applied a tip voltage pulse while holding the gate voltage at V_g = −20 V. Figure 3c shows a dI/dV map of the same region after applying the tip pulse. The most striking feature in the dI/dV map after the tip pulse is the emergence of a red disk region in the upper right quadrant of the map, which also exhibits a darkened halo around the perimeter. Although only one quadrant is shown, the new red region exhibits rough circular symmetry. The altered charge landscape is stable at T = 5 K long after the pulse has been applied, but it can be erased by application of an identical tip pulse with the gate voltage held at V_g = 0 V. Figure 3d shows a dI/dV image of the same graphene patch after application of such an "eraser" pulse. The altered red disk is now completely gone and the graphene is returned to its pristine state.

The new charge-doping landscape induced by the tip pulse can be explained by a combination of field-induced defect ionization and charge diffusion within the BN insulator (see Supporting Information for more discussion on BN defects). The strong electric field of the tip pulse penetrates through the gated graphene into the insulator region (previous studies have also shown similar electric field penetration through gated graphene[26]), causing a strong potential gradient around BN defects and resulting in enhanced defect field emission. When the gate is on during a tip pulse, the gate electric field causes released electrons to drift either into the graphene electrode (V_g < 0, resulting in a positive space charge layer in the BN) or away from the graphene electrode (V_g > 0, resulting in a negative space charge layer in the BN). Pulses applied with V_g = 0 V allow charge to freely diffuse and recover the initial state of graphene. The net result is that both p-type and n-type doping profiles can be written and erased in pristine graphene/BN with a spatial resolution determined by the potential gradient surrounding an STM tip. For example, the red region in Figure 3c is n-doped graphene while the blue region surrounding it is p-doped graphene (see Figure S3), and the boundary between these two regions defines a rewritable nanoscale p−n junction (we have also performed transport measurements that clearly demonstrate the creation of a graphene p−n junction using our tip-doping technique (Figure S4)).

The strong similarities in phenomenology between both the light-induced and tip-pulsing-induced doping modalities described here suggest that they might even be combined. To demonstrate this compatibility, we show how a localized n-doped region can be "written" into a p-doped background and then erased by optical excitation. Figure 4a shows a dI/dV map

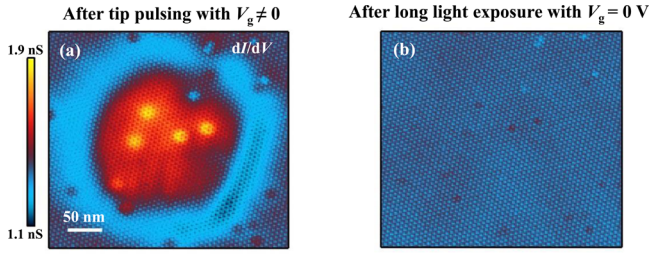

Figure 4. Doping patterns written by an STM tip and erased by light. (a) The dI/dV map of graphene/BN after applying a tip pulse at the center, while holding V_g = −20 V (I = 0.4 nA, V_s = −0.25 V, $\tilde{V}_g$ = −15 V). (b) The dI/dV map of the same region after extended light exposure (30 min) while holding V_g = 0 V (same tunneling parameters as (a)). All data were acquired from a device with a 44 μm width and 39 μm source-drain separation.

of an n-doped region (∼200 nm across) created through application of a tip pulse at the center of the image, while holding the gate voltage at V_g = −20 V. Light-induced erasure of this pattern was subsequently performed by exposing the sample to light for 30 min, while holding the gate voltage at V_g = 0 V. Figure 4b shows a dI/dV map of the same region after the erasure process. The red n-doped region is clearly absent, demonstrating that light exposure can erase doping patterns fabricated via tip pulses. These observations show that combined tip and optical-induced charge doping is a flexible scheme for creating rewritable p−n junctions of arbitrary geometry.

In the present work, we have demonstrated writing, reading, and erasing of artificial doping patterns at the nanoscale in pristine graphene/BN heterostructures. Our local patterning method uses light or voltage pulses to liberate charge from BN defects, which is then guided by the gate electric field. This simple and clean defect-based lithography method provides flexibility both for writing and erasing operations. The ultimate spatial resolution of this technique will depend on the geometry of the probe tip, which could be enhanced through the use of high aspect-ratio structures such as nanotubes. Our charge-doping control scheme may also be employed on other types of

DOI: 10.1021/acs.nanolett.5b04441
Nano Lett. 2016, 16, 1620−1625

low-dimensional heterostructures, such as transition metal dichalcogenides and flexible memory cells.[27,28]

Methods. Our samples were fabricated using a transfer technique developed by Zomer and colleagues[29] that employs standard electron-beam lithography. We used high purity BN crystals synthesized by Taniguchi et al.[30] and exfoliated to 60−100 nm thickness with SiO_2 thicknesses of 300 or 285 nm used as the dielectric for electrostatic gating. Monolayer graphene was exfoliated from graphite and deposited onto methyl methacrylate (MMA) polymer and transferred onto BN (that was also annealed before graphene was transferred onto it) supported by an SiO_2/Si wafer. Completed devices were subsequently annealed in flowing Ar/H_2 forming gas at 350 °C and their electrical conductance was measured with a standard ac voltage bias lock-in technique with a 50 μV signal at 97.13 Hz. A fiber-based super continuum laser was guided into a (T = 77 K) cryostat through an optical window for the transport measurements presented in Figure 2a. Samples that exhibited bipolar transport within a gate voltage range of −30 to 30 V were transferred into our Omicron ultrahigh vacuum (UHV) low-temperature STM. A second anneal was then performed for several hours at ∼300 °C and 10^{-11} Torr before moving the device into the STM chamber for measurements at T = 5 K. Before all STM measurements our platinum iridium STM tip was calibrated by measuring the Shockley surface state of an independently cleaned Au(111) crystal. All STM images were acquired in a constant current mode with $-V_s$ applied to the STM tip relative to a grounded sample. All scanning tunneling spectroscopy (STS) measurements were obtained by lock-in detection of the ac tunnel current induced by a modulated voltage (6−10 mV at 613.7 Hz) added to V_s. A diode laser (405 nm wavelength) and an Ar ion laser (454−514 nm wavelength) that are external to the STM were used for light exposure before the acquisition of the dI/dV maps presented in Figure 2 c−e.

■ ASSOCIATED CONTENT

Supporting Information

The Supporting Information is available free of charge on the ACS Publications website at DOI: 10.1021/acs.nanolett.5b04441.

(1) Determination of $\tilde{V}_g$ for light-induced doping, (2) procedure for converting dI/dV intensity to charge density fluctuations after light-induced doping, (3) tip-doping dI/dV spectra for $V_g > 0$ V, (4) conversion of dI/dV intensity to charge density after tip-doping, (5) detailed tip-doping procedure, (6) $G(V_g)$ transport data before and after tip-doping, and (7) discussion of the nature of the BN defects. (PDF)

■ AUTHOR INFORMATION

Corresponding Author

*E-mail:crommie@berkeley.edu.

Present Address

(J.L.) Department of Chemistry, National University of Singapore, 3 Science Drive 3, Singapore 117543 and Centre for Advanced 2D Materials and Graphene Research Centre, National University of Singapore, 6 Science Drive 2, Singapore 117546.

Author Contributions

J.V.J., L.J., and D.W. contributed equally to this manuscript. J.V.J., L.J., and D.W. conceived the work and designed the research strategy. J.V.J. and D.W. performed data analysis. J.V.J., S.K., L.J., and A.Z. facilitated sample fabrication. D.W., J. Lee, and J.V.J. carried out STM/STS measurements. J.V.J., L.J., and S.K. carried out electron transport measurements. L. J. constructed the optical setup. K.W. and T.T. synthesized the h-BN samples. D.W., J.V.J., and L.J. formulated theoretical model with advice from M.F.C. M.F.C. supervised the STM/STS experiments. J.V.J., L.J., D.W., and M.F.C. cowrote the manuscript. J.V.J. and M.F.C. coordinated the collaboration. All authors discussed the results and commented on the paper.

Notes

The authors declare no competing financial interest.

■ ACKNOWLEDGMENTS

The authors thank P. Yu, J. Jung, and A. Rubio for stimulating discussions and S. Onishi for help with the scanning electron microscope. This research was supported by the Director, Office of Science, Office of Basic Energy Sciences of the U.S. Department of Energy under contract no. DE-AC02-05CH11231 (sp2 program) (STM imaging and spectroscopy) and National Science Foundation Grant DMR-1206512 (sample fabrication). D.W. was supported by the Department of Defense (DoD) through the National Defense Science and Engineering Graduate Fellowship (NDSEG) Program, 32 CFR 168a. K.W. and T.T. acknowledge support from the MEXT Japan Elemental Strategy Initiative (synthesis of BN crystals) and JSPS Grant-in-Aid for Scientific Research on Innovative Areas no. 25107004 (characterization of BN crystals). T.T. acknowledges support from a JSPS Grant-in-Aid for Scientific Research on Innovative Areas no. 25106006 (development of high-pressure BN synthesis instrumentation). J. Lu acknowledges the National Research Foundation, CRP award "Novel 2D materials with tailored properties: beyond graphene" (R-144-000-295-281).

■ REFERENCES

(1) Cheianov, V. V.; Fal'ko, V.; Altshuler, B. L. *Science* **2007**, *315* (5816), 1252−1255.
(2) Williams, J. R.; Low, T.; Lundstrom, M. S.; Marcus, C. M. *Nat. Nanotechnol.* **2011**, *6* (4), 222−225.
(3) Young, A. F.; Kim, P. *Nat. Phys.* **2009**, *5* (3), 222−226.
(4) Zhao, Y.; Wyrick, J.; Natterer, F. D.; Rodriguez-Nieva, J. F.; Lewandowski, C.; Watanabe, K.; Taniguchi, T.; Levitov, L. S.; Zhitenev, N. B.; Stroscio, J. A. *Science* **2015**, *348* (6235), 672−675.
(5) Baugher, B. W. H.; Churchill, H. O. H.; Yang, Y.; Jarillo-Herrero, P. *Nat. Nanotechnol.* **2014**, *9* (4), 262−267.
(6) Ross, J. S.; Klement, P.; Jones, A. M.; Ghimire, N. J.; Yan, J.; Mandrus, D. G.; Taniguchi, T.; Watanabe, K.; Kitamura, K.; Yao, W.; Cobden, D. H.; Xu, X. *Nat. Nanotechnol.* **2014**, *9* (4), 268−272.
(7) Pospischil, A.; Furchi, M. M.; Mueller, T. *Nat. Nanotechnol.* **2014**, *9* (4), 257−261.
(8) Vakil, A.; Engheta, N. *Science* **2011**, *332* (6035), 1291−1294.
(9) Williams, J. R.; DiCarlo, L.; Marcus, C. M. *Science* **2007**, *317*, 638−641.
(10) Ozyilmaz, B.; Jarillo-Herrero, P.; Efetov, D.; Abanin, D. A.; Levitov, L. S.; Kim, P. *Phys. Rev. Lett.* **2007**, *99*, 166804.
(11) Huard, B.; Sulpizio, J. A.; Stander, N.; Todd, K.; Yang, B.; Goldhaber-Gordon, D. *Phys. Rev. Lett.* **2007**, *98*, 236803.
(12) Liu, G.; Velasco, J.; Bao, W. Z.; Lau, C. N. *Appl. Phys. Lett.* **2008**, *92* (20), 203103.
(13) Lohmann, T.; von Klitzing, K.; Smet, J. H. *Nano Lett.* **2009**, *9* (5), 1973−1979.
(14) Velasco, J.; Liu, G.; Bao, W. Z.; Lau, C. N. *New J. Phys.* **2009**, *11*, 095008.

DOI: 10.1021/acs.nanolett.5b04441
Nano Lett. 2016, 16, 1620−1625

(15) Crook, R.; Graham, A. C.; Smith, C. G.; Farrer, I.; Beere, H. E.; Ritchie, D. A. *Nature* **2003**, *424* (6950), 751−754.
(16) Ju, L.; Velasco, J., Jr.; Huang, E.; Kahn, S.; Nosiglia, C.; Tsai, H.-Z.; Yang, W.; Taniguchi, T.; Watanabe, K.; Zhang, Y.; Zhang, G.; Crommie, M.; Zettl, A.; Wang, F. *Nat. Nanotechnol.* **2014**, *9* (5), 348−352.
(17) Dean, C. R.; Young, A. F.; Meric, I.; Lee, C.; Wang, L.; Sorgenfrei, S.; Watanabe, K.; Taniguchi, T.; Kim, P.; Shepard, K. L.; Hone, J. *Nat. Nanotechnol.* **2010**, *5* (10), 722−726.
(18) Adam, S.; Hwang, E. H.; Galitski, V. M.; Das Sarma, S. *Proc. Natl. Acad. Sci. U. S. A.* **2007**, *104* (47), 18392−18397.
(19) Du, X.; Skachko, I.; Barker, A.; Andrei, E. Y. *Nat. Nanotechnol.* **2008**, *3* (8), 491−495.
(20) Wong, D.; Velasco, J., Jr.; Ju, L.; Lee, J.; Kahn, S.; Tsai, H. Z.; Germany, C.; Taniguchi, T.; Watanabe, K.; Zettl, A.; Wang, F.; Crommie, M. F. *Nat. Nanotechnol.* **2015**, *10* (11), 949−953.
(21) Zhang, Y.; Brar, V. W.; Girit, C.; Zettl, A.; Crommie, M. F. *Nat. Phys.* **2009**, *5* (10), 722−726.
(22) Deshpande, A.; Bao, W.; Miao, F.; Lau, C. N.; LeRoy, B. J. *Phys. Rev. B: Condens. Matter Mater. Phys.* **2009**, *79*, 205411.
(23) Xue, J.; Sanchez-Yamagishi, J.; Bulmash, D.; Jacquod, P.; Deshpande, A.; Watanabe, K.; Taniguchi, T.; Jarillo-Herrero, P.; LeRoy, B. J. *Nat. Mater.* **2011**, *10* (4), 282−285.
(24) Decker, R. g.; Wang, Y.; Brar, V. W.; Regan, W.; Tsai, H.-Z.; Wu, Q.; Gannett, W.; Zettl, A.; Crommie, M. F. *Nano Lett.* **2011**, *11* (6), 2291−2295.
(25) Zhang, Y. B.; Brar, V. W.; Wang, F.; Girit, C.; Yayon, Y.; Panlasigui, M.; Zettl, A.; Crommie, M. F. *Nat. Phys.* **2008**, *4* (8), 627−630.
(26) Britnell, L.; Gorbachev, R. V.; Jalil, R.; Belle, B. D.; Schedin, F.; Mishchenko, A.; Georgiou, T.; Katsnelson, M. I.; Eaves, L.; Morozov, S. V.; Peres, N. M. R.; Leist, J.; Geim, A. K.; Novoselov, K. S.; Ponomarenko, L. A. *Science* **2012**, *335* (6071), 947−950.
(27) Sup Choi, M.; Lee, G.-H.; Yu, Y.-J.; Lee, D.-Y.; Hwan Lee, S.; Kim, P.; Hone, J.; Jong Yoo, W. *Nat. Commun.* **2013**, *4*, 1624.
(28) Bertolazzi, S.; Krasnozhon, D.; Kis, A. *ACS Nano* **2013**, *7* (4), 3246−3252.
(29) Zomer, P. J.; Dash, S. P.; Tombros, N.; van Wees, B. J. *Appl. Phys. Lett.* **2011**, *99* (23), 232104−232107.
(30) Taniguchi, T.; Watanabe, K. *J. Cryst. Growth* **2007**, *303* (2), 525−529.

DOI: 10.1021/acs.nanolett.5b04441
Nano Lett. 2016, 16, 1620−1625